International Journal of Nanomedicine

Dovepress

open access to scientific and medical research

Open Access Full Text Article

ORIGINAL RESEARCH

Perampanel Reduces Brain Damage via Induction of M2 Microglia in a Neonatal Rat Stroke Model

Hyo Jung Shin[1,2,*], Ka Young Lee[1,3,*], Joon Won Kang[4,5], Seung Gyu Choi[1,5], Dong Woon Kim[1,2,4,*], Yoon Young Yi[6,*]

[1]Department of Anatomy and Cell Biology, Chungnam National University, Daejeon, Republic of Korea; [2]Brain Research Institute, Chungnam National University, Daejeon, Republic of Korea; [3]Department of Rehabilitation Medicine, Seoul National University Bundang Hospital, Seongnam, Republic of Korea; [4]Department of Medical Science, Chungnam National University, Daejeon, Republic of Korea; [5]Department of Pediatrics, Chungnam National Hospital, School of Medicine, Chungnam National University, Daejeon, Republic of Korea; [6]Department of Pediatrics, College of Medicine, Hallym University and Gangdong Sacred Heart Hospital, Seoul, Republic of Korea

*These authors contributed equally to this work

Correspondence: Dong Woon Kim; Yoon Young Yi, Tel +82-42-580-8207; +82-2-2224-2251, Email visnu528@cnu.ac.kr; 070133@kdh.or.kr

Purpose: Ischemic stroke is a leading cause of death and disability worldwide. Additionally, neonatal ischemia is a common cause of neonatal brain injury, resulting in cerebral palsy with subsequent learning disabilities and epilepsy. However, there is currently a lack of effective treatments available for patients with perinatal ischemic stroke. In this study, we investigated the effect of perampanel (PER)-loaded poly lactic-co-glycolic acid (PLGA) by targeting microglia in perinatal stroke.

Methods: After formation of focal ischemic stroke by photothrombosis in P7 rats, PER-loaded PLGA was injected intrathecally. Proinflammatory markers (TNF-α, IL-1β, IL-6, COX2, and iNOS) and M2 polarization markers (Ym1 and Arg1) were evaluated. We investigated whether PER increased M2 microglial polarization in vitro.

Results: PER-loaded PLGA nanoparticles decreased the pro-inflammatory cytokines compared to the control group. Furthermore, they increased M2 polarization.

Conclusion: PER-loaded PLGA nanoparticles decreased the size of the infarct and increased motor function in a perinatal ischemic stroke rat model. Pro-inflammatory cytokines were also reduced compared to the control group. Finally, this development of a drug delivery system targeting microglia confirms the potential to develop new therapeutic agents for perinatal ischemic stroke.

Keywords: ischemic stroke, neonate, poly lactic-*co*-glycolic acid, PLGA, nanoparticle, perampanel, microglial polarization

Introduction

Perinatal ischemic stroke occurs in 1 per 4000 live births[1] and causes significant morbidity and severe long-term neurologic sequelae in children. The pathophysiology of perinatal stroke may often relate to the unique environmental factors that surround the time of birth, with a relatively low recurrence rate, in contrast to adult cases.[2] For the treatment of ischemic stroke, recanalization of blood vessels with thrombolytic or endovascular treatments can be helpful.[3,4] However, this has a narrow therapeutic window of 4.5 hours from the onset of a stroke in certain eligible patients, and it is currently rarely performed in newborns.[5] Thus, there is still no standard acute therapy available for perinatal stroke, and the focus is on supportive treatment and neuroprotection. It is important to investigate effective treatments for perinatal ischemic stroke.

In response to ischemic stroke, microglia are activated and polarized to the pro-inflammatory M1 phenotype or the anti-inflammatory M2 phenotype. Also, pro-inflammatory M1 microglia, as the primary source of cytokines and free radicals, can induce secondary brain damage.[6] Control of microglial polarization can be an important therapeutic strategy. The immunomodulatory molecules generated by these microglia, such as cytokines and chemokines, are closely associated with secondary brain damage or repair, respectively, following ischemic stroke. In the MCAO-induced ischemic stroke model, M1 phenotype microglia were increased, and ischemic lesions induced microglial inflammation

Received: 6 February 2022
Accepted: 18 June 2022
Published: 27 June 2022

Graphical Abstract

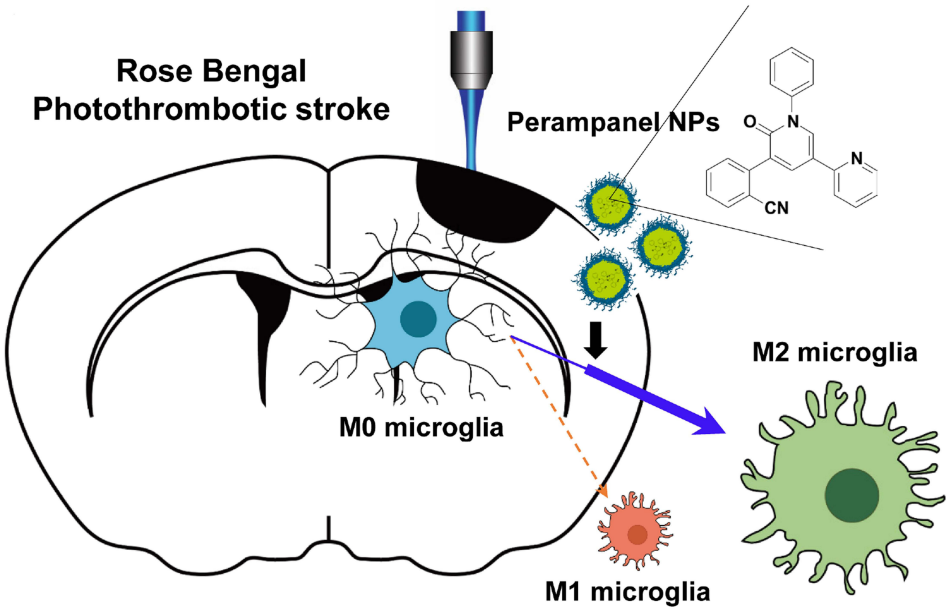

in the ipsilateral cortex.[7] Therefore, investigating microglial changes and their functions is crucial to understanding ischemic stroke pathophysiology.

Nanoparticles have been widely applied in biomedical fields for use in diagnosis, biosensing, and drug delivery. Recently, many nanoparticles have been reported to be useful vehicles for delivery of drugs to inhibit the over-activation of microglia and neuro-inflammation.[8,9] Biodegradable polymeric nanoparticles such as poly lactic-*co*-glycolic acid (PLGA) and poly lactic acid (PLA) have been well studied as stable drug carriers for drug delivery. Among them, PLGA has proven to be effective as a drug delivery method for gene regulators such as siRNAs, plasmids, and miRNA.[10–12] PLGA nanoparticles (NPs) have also been approved for pharmaceutical application by the US Food and Drug Administration.[13] Moreover, recent studies have shown that PLGA NPs are preferentially localized to microglia.[14] Among the cells in CNS, microglia were shown to take up 63.41% of rhodamine-conjugated PLGA NPs at 24 hours.[8,15]

Perampanel (PER) is a noncompetitive α-amino-3-hydroxyl-5-methyl-4-isoxazolepropionate (AMPA) receptor antagonist that is clinically used for seizure control. AMPA receptors are postsynaptic ionotropic excitatory receptors with binding sites for glutamate that are thought to participate in the induction of seizures by synchronizing excitatory glutamatergic signaling.[16] In preclinical studies, PER was found to be effective in preventing seizures in a seizure model,[17] and was studied in vitro as an inhibitor of the dose-dependent AMPA-mediated increase in intracellular calcium.[18] Moreover, recent studies have reported that PER has neuroprotective effects in experimental models of stroke[19,20] and traumatic brain injury.[21] The AMPA receptor, the target of PER, is present not only in neurons but also in activated microglia.[22] By examining the action on the AMPA receptor of PER contained in nanoparticles with high affinity for microglia, it may be possible to target this receptor for perinatal stroke treatment. There is still no research of the action of PER on microglia for the treatment of perinatal stroke. Based on the distribution of drug-loaded PLGA NPs, it is reasonable to hypothesize that PER-loaded NPs will influence microglia directly. In the present study, we investigated the effects of PER-loaded NPs on microglial polarization in a perinatal ischemic stroke rat model.

Materials and Methods

Photothrombotic Stroke Animal Model

All experiments were approved by the Animal Care and Use Committee at Chungnam National University Hospital (CNUH-020-A0049, 19 Nov 2020) and were consistent with the ethical guidelines of the National Institutes of Health. P7

Sprague-Dawley rats purchased from The Damul Science (Daejeon, Korea) were used for all experiments. All experiments were approved by the Animal Care and Use Committee at Chungnam National University Hospital (CNUH-020-A0049, 19 Nov 2020) and were consistent with the ethical guidelines of the National Institutes of Health. Rats were housed at 23°C under a controlled 12-hour:12-hour light: dark cycle, with the light on at 08:00.

To induce photothrombosis, the photosensitive dye Rose Bengal (RB; Sigma, St. Louis, MO, USA) was dissolved in phosphate-buffered saline (PBS) and injected intraperitoneally (i.p.) at a dose of 25 mg/kg. Thirty minutes after injection, the rats were placed in the prone position on an operating table under 3% isoflurane anesthesia in air and oxygen during the surgical procedure. Then, blue light (560 nm) from an LED lamp (Zeiss, CL6000) was focused on the right cerebral cortex for 1 minute to aggregate the dye. PER or PBS encapsulated in PLGA NPs was injected into the cisterna magna immediately after RB-induced photothrombosis. The 20-μL solutions of NPs were injected using a 100-μL syringe (Hamilton, Reno, NV, USA) equipped with a 26G needle.

Triphenyltetrazolium Chloride Staining and Infarct Volume Measurement

Rats were sacrificed at 24 h after photothrombosis, we collected the tissue. The brain was washed in cold PBS for 5 minutes and was cut into 2-mm-thick coronal sections in a cutting block. Then, brain slices were stained with 1% Triphenyltetrazolium chloride (TTC) (Sigma, St. Louis, MO, USA) at 37°C for 30 minutes in the dark, followed by 4% paraformaldehyde. Infarct volume was calculated by the trapezoidal rule using Image J (National Institutes of Health) as previously described.[23] Total infarction volume was taken to be the sum of the core and penumbra volumes. Damage volume was calculated as the percentage of ipsilateral hemisphere volume.

Histological Examination

The brain tissues from rats were embedded in paraffin. Serial coronal sections were produced and mounted on slides. The specimens were stained with hematoxylin and eosin (H&E) and cresyl violet according to standardized protocols, and visualized by light microscopy.

Wire Hang Test

Neurological deficits were assessed using the hanging test. The behavioral tests were performed by blinded observers immediately before and one day after photothrombosis. The time from when both of the rat's forelimbs were hung on a 3 mm wire until falling off was measured. A wire cage (18 in. × 9 in.) without a lid on the top was used for this experiment. This test was repeated three times, with an interval of 3 minutes between attempts.

Synthesis and Characterization of per Encapsulated in PLGA Nanoparticles

PLGA NPs with a 50:50 ratio of lactic and glycolic acids and carrying PER or PBS were prepared using an emulsification/solvent evaporation method.[11] PER (10 mg) was dissolved in PBS at a concentration of 0.1%, and diluted in PBS to a final concentration of 1 mg/200 μL, then added in a dropwise manner to 800 μL dichloromethane containing 25 mg of PLGA (Corbion, Amsterdam, the Netherlands). The mixture was emulsified using sonication (Branson Digital Sonifier, SFX 550, EMERSON, Danbury, CT, USA) into a primary W1/O emulsion. Then, 2 mL 1% PVA1500 was added directly to the primary emulsion, and further emulsified by sonication to form a W1/O/W2 double emulsion. Physical characteristics of the NPs were analyzed with the Zetasizer Nano ZS90 (Malvern Instruments, Enigma Business Park, Grovewood Road, UK).[24] The diameter and shape were evaluated using SEM (SNE-4500 M; SEC Co., Ltd., Suwon, Republic of Korea).

Drug Loading Efficiency and Encapsulation Efficiency

PER NPs were completely dissolved in DMSO at 5 mg/mL concentration. PER concentration was calculated based on 595 nm absorbance under ELISA (Sunrise, TECAN). The encapsulation efficiency (EC) for the direct analysis was calculated using the following equations: EC (%) = (Measured released drugs/Initially loaded drugs) × 100. Loading efficiency (%) = (released drug after completed hydrolysis/total amount of NPs) x100 .

Drug Release Assay

To classify the drug release, each 2.5 mg of drug-encapsulated PLGA nanoparticles were collected and incubated in an Eppendorf tube with 250 μL of phosphate buffered saline (PBS) pH 7.4 at 37°C. At the designated time, 200 μL of the supernatant was taken and replaced by the same amount of a fresh buffer. PER concentration was calculated based on 595 nm absorbance under ELISA (Sunrise, TECAN).

Quantitative Polymerase Chain Reaction (qPCR)

Total RNA was isolated from the cortex of the ipsilateral hemisphere using TRIzol reagent according to the manufacturer's protocol (GeneAll, RoboEx^{TM}, Thermo Fisher Scientific, Waltham, MA, USA). RNA quality was evaluated spectrophotometrically using a NanoDrop LITE (Thermo Fisher Scientific, Evolution 201). Reverse transcription was performed with 10 μg of total RNA in a total reaction volume of 30 μL using a kit (Enzynomics, Daejeon, Korea). qPCR was performed using the AriaMx Real-Time PCR system (Agilent Technologies, Santa Clara, CA, USA) with the TOPreal^{TM} qPCR 2× premix (SYBR Green with lox ROX; Enzynomics). The primers used for mouse GAPDH, TNF-α, IL-1β, COX2, IL-6, iNOS, and Arg1 were as follows: rGAPDH 5'-CTCAT GACCACAGTCCATGC-3', and antisense 5'-TTCAGCTCTGGGATGACCTTCT-3'; rTNF-α 5'-AG CAAACCACCAAGTGGAGGA-3' and antisense 5'-GCTGGCACCACTAGTTGGTTGT-3'; rIL-1β 5' -TTGTGGCTGTGGAGAAGCTGT-3' and antisense 5'-AACGT CACACACCAGCAGGTT-3'; rCOX2 5'-TGAGTACCGCAAACGCTTCT-3' and antisense 5'-CTCCCCAAA GATAGCATCTGG -3'; rIL-6 5'-TCCATCCAGTTGCCTTCTTGG-3' and antisense 5'-CCACGATTTCCCAGA GAACAT G-3'; riNOS 5'-GGCAAACCCAAGGTCTACGTT-3' and antisense 5'-TCGCTCAAGTTCAGCTTG GT-3'; mArg1 5'-CTTCAGAGAAGTGGCCCAAC-3' and antisense 5'-GGTGGTGGGTATCACAG GAC-3'; mGAPDH 5'-ACCCAGAAGACTGTGGATGG-3', and antisense 5'-CACATTGGGGGTAG GAACAC-3'. The mRNA level of each target gene was normalized to that of GAPDH mRNA. The fold-changes in the mRNA levels were calculated using the $2^{-\Delta\Delta Ct}$ method as previously described.[23]

Cell Viability Assay

The BV2 immortalized murine microglial cell line was received from Dr Joe EH at Ajou University.[25] Blasi et al generated BV-2 cells by infecting primary microglia with a v-raf/v-myc oncogene carrying retrovirus (J2) and confirmed that BV-2 cells retain most of the morphological, phenotypical and functional properties of freshly isolated microglia.[26] The BV2 cell line was grown in Dulbecco's modified Eagle's medium (DMEM) with 10% fetal bovine serum. All cultures were kept at 37°C in a 5% CO2 humidified incubator. To determine the cytotoxicity of PER itself and of PER NPs, cell viability assays were performed using the EZ-Cytox cell viability assay kit (Daeil Lab Service, Seoul, Korea) according to the manufacturer's instructions.

Immunohistochemistry and Western Blotting

Immunohistochemistry and immunoblotting were performed as previously described.[8] For immunocytochemistry, 30-μm sections of brain tissue were incubated with a blocking buffer (5% normal chicken serum/0.3% Triton X-100 in PBS) for 1 h, and were immunostained with antibodies against Iba-1 (Wako, Richmond, USA), NeuN (Millipore, Billerica, MA, USA), and GFAP (DAKO, Glostrup, Denmark) overnight. Nucleus staining was performed with DAPI (H3570, Invitrogen). Click-iT TUNEL Alexa Fluor 488 Imaging Assay (Thermo Fisher Scientific, C10245) was used to analyze apoptosis according to the manufacturer's instructions.[27] An Axiophot microscope (Carl Zeiss, LSM900) was used for the analysis of double-stained sections. The immunodenstities in the graphs were quantified using ImageJ. For Western blotting, samples were prepared by cutting only 7 mm of the infarct lesion of the hemisphere cortex. The antibodies were rabbit anti-Ym1 (BAF2446, 1:500, R&D Systems), anti-Arg1 (sc-271430, 1:500, Santa Cruz), anti-Iba-1 (NB100-1028, 1:500, Novus), anti-CD206 (ab64693, 1:500, Abcam), and anti-ACTB (A5316, 1:500, Sigma). After 24 hours RB modelling, for Hematoxylin and eosin staining, the brains were embedded in paraffin and coronal sections (of 4 μm thickness) were sliced and stained with H&E. The cerebral cortex at the same level of each group were observed the morphology changes under a light microscope (Olympus AX70, Japan).

Statistical Analyses

All the data are represented in the text and figure legends as mean ± SEM. Statistical differences between more than two groups were analyzed using one-way ANOVA followed by Tukey's post hoc analysis. The statistical differences between two groups were determined by the paired Student's *t*-test. All data are representative of at least three independent experiments. A value of *P* less than 0.05 was considered statistically significant. All statistical analyses were conducted using Prism 9.0 software (GraphPad, San Diego, CA, USA).

Results

Microglial Activation After Focal Ischemic Stroke Induced by Photo-Thrombosis

To generate the focal ischemic stroke model in neonatal rats, RB was injected i.p. (25 mg/kg) in P7 rats. Thirty minutes after injection, photothrombosis was induced in the RB group with blue laser light for 1 minute (Figure 1A). The wire hanging time was shorter in the RB-injected group (n = 6; 6.67 ± 0.88) than in the control group (n = 6; 15.50 ± 0.50, $P < 0.0001$). For the observed infarct area, a volume of 9.000 ± 0.6831 (n = 6, $P < 0.0001$) could be confirmed in the RB-injected group (Figure 1B). Histological changes in photochemically induced stroke were evaluated by TTC staining. A selective focal ischemic lesion in the right sensorimotor cortex area was revealed after TTC staining (Figure 1C). The TTC-negative region was significantly well demonstrated on the first day after stroke induction. When we stained the neonatal rat brain for the microglial marker Iba-1, activated forms of microglia were abundant (Figure 1D). Microglial cells are continually activated by pro-inflammatory stimuli. These chronically activated microglia will continue to produce inflammatory cytokines, which could lead to neuronal death. Indeed, to investigate whether microglial activation progressed and whether cytokine release was increased, the time-dependent mRNA expression of pro-inflammatory genes was investigated after RB modeling. mRNA expression of TNF-α, IL-1β, COX2, IL-6, and iNOS increased after stroke occurrence (Figure 1E). These data demonstrate that microglia were activated in cortical infarcts by RB-induced photothrombotic stroke, and also that neuroinflammation increased in the neonatal stroke rat model.

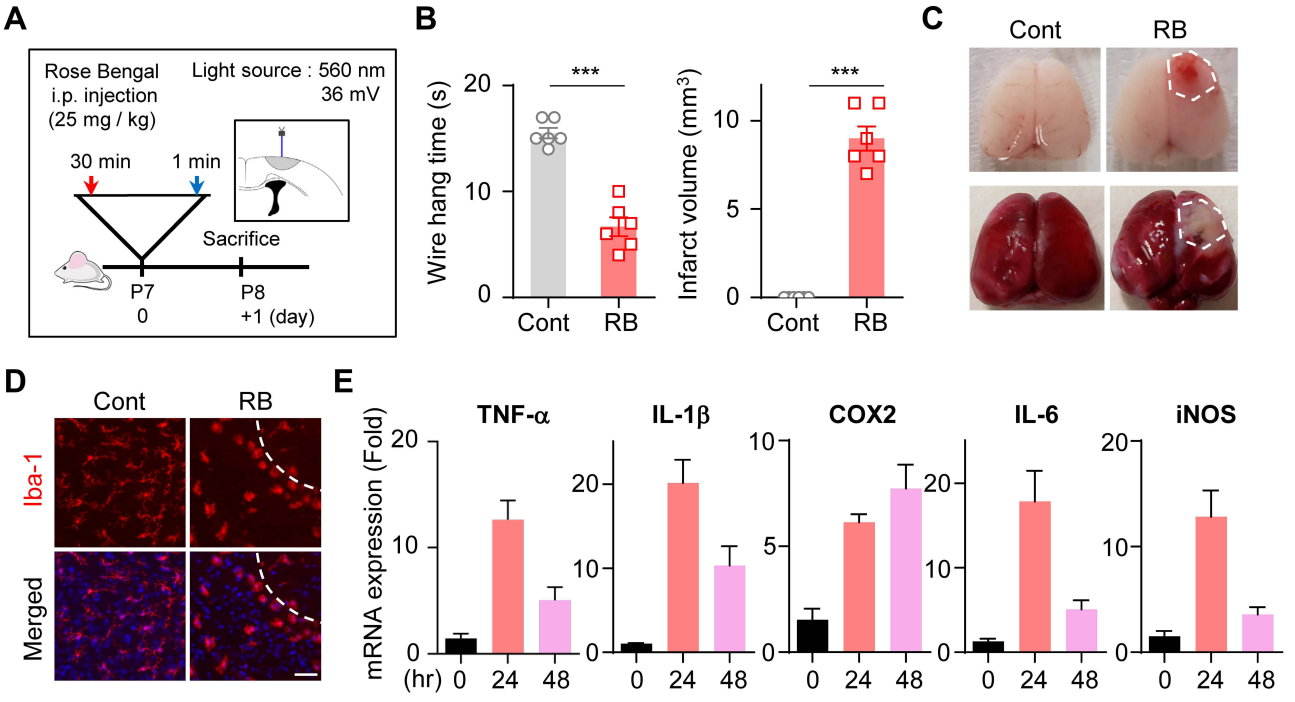

Figure 1 Microglia activation and cytokine release in RB photothrombosis: (**A**) Photothrombosis is achieved via i.p. injection of RB and illumination of the sensory motor cortex through a cranial window. (**B**) Quantification of infarct volume and wire hang test. (**C**) Representative photographs of whole brain stained with TTC, and whole brain 24 hours after initiating the model. (**D**) Brain tissues were immunostained with anti-Iba-1 antibodies. (**E**) Total RNA was isolated from the infarct region of the ipsilateral brain, and used for cDNA synthesis. The mRNA levels of TNF-α, IL-1β, Cox2, IL-6, and iNOS were determined by qRT-PCR in all groups.
Notes: (**B**–**E**) Data represented as mean ± SEM. (**B**) ***$P < 0.01$ compared with the control group. (**D**) Scale bar = 200 μm.
Abbreviations: RB, Rose Bengal; i.p., intraperitoneally; SEM, standard error of mean; TTC, Triphenyltetrazolium chloride.

AAV-EF1α-mCherry Vector Encapsulated in PLGA Nanoparticles Was Predominantly Taken Up into Microglia

As our research group reported previously that PLGA NPs were preferentially taken up into microglia,[8,15] it was necessary to determine the types of cells in which PER NPs would mainly be located in the brains of neonatal rats. The AAV-EF1α-mCherry vector encapsulated in particles was prepared for tracking cellular uptake by the emission of mCherry red fluorescence. AAV-EF1α-mCherry vector-loaded PLGA NPs were injected into the cisterna magna through the intervertebral space, using a Hamilton syringe. After three days, brain sections were immunostained for cell type-specific markers with anti-Iba-1 (microglia marker), anti-NeuN (neuronal marker), and anti-GFAP (astrocyte marker) antibodies. The 3D reconstruction result was obtained from a confocal image using the IMARIS program. The mCherry images showed overlapping red fluorescence of each cell-specific marker, and only the designated fluorescence was imaged (Figure 2A). Although AAV-EF1α-mCherry vector NPs were observed in all cell types, 59 ± 7.8% of mCherry expression co-localized with microglia, 14.08 ± 3.52% was observed in astrocytes, and 26.59 ± 6.71% was observed in neurons (Figure 2B). As a result, twice as much mCherry fluorescence was detected in microglia present in the sensory motor cortex as in other glial cells. Nanoparticles with AAV-EF1α-mCherry vector were taken up by all cell types, but most were taken up by microglia, in which phagocytosis is most active.

Characterization and Preparation of per-Loaded PLGA Nanoparticles

By ELISA, levels of the pro-inflammatory cytokines TNF-α and Il-1β were reduced by PER in brain tissue and serum. In acute ischemic stroke, PER therapy reduces neuroinflammation, oxidative stress, and apoptotic activity. Notably, PER ameliorates post-stroke cognitive impairment through reduction in neuronal damage.[19] PER is the first highly selective and non-competitive AMPA-type glutamate receptor antagonist available on the drug market. In addition, AMPA receptors are widely distributed, expressed not only in neurons but also in glial cells, especially microglia. Therefore, a study on the mechanism by which PER works by targeting microglia suggested that it could be applied as a new therapeutic agent.[22,28] PER is expected to more effectively increase the neuroprotective effect by acting on microglia. Also, we intended to study the mechanism of action of microglia by using the advantage that PLGA NPs are mainly taken up into microglia.

To deliver PER predominantly to microglia, we applied PLGA as a drug-delivery tool. In order to check the cellular location of action, PLGA with rhodamine fluorescence was produced (Figure 3A). PER NPs were characterized with a Zetasizer, and shown to have an average particle size of 216.7 nm and zeta potential of –40.9 mV (Figure 3B and C). After preparation of rhodamine-conjugated PER-loaded PLGA NPs, we observed that BV2 cells engulfed rhodamine

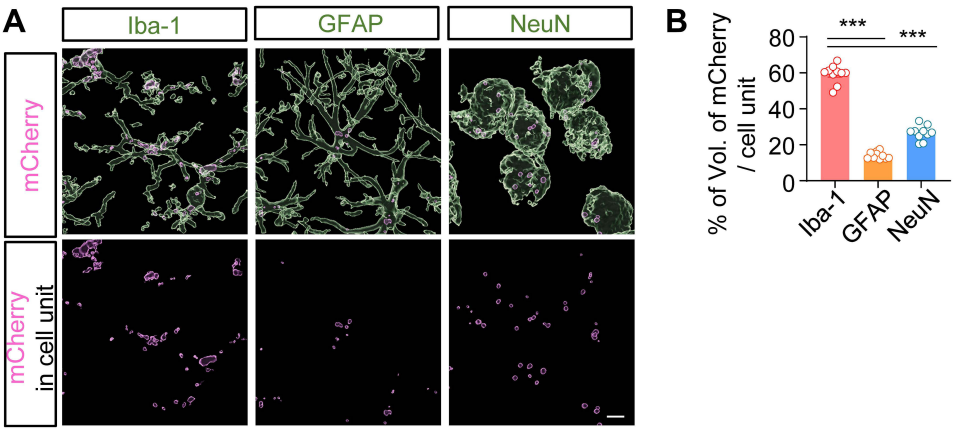

Figure 2 AAV-EF1α-mCherry-PLGA NPs were i.t. administered to cisterna magna: (**A**) On day 3 after injection, tissue of brain was isolated and used for immunostaining with anti-Iba-1, GFAP, and NeuN antibodies. The images of red fluorescence were obtained only with the expression of mCherry observed in each cell type. (**B**) The volume of mCherry fluorescence was quantified using the IMARIS program.

Notes: (**B**) Data are presented as the mean ± SEM, analyzed by one-way ANOVA followed by Tukey's post hoc test, ***$P < 0.01$ compared with the other cell type.

Abbreviations: AAV, adenovirus vector; PLGA, poly lactic-*co*-glycolic acid; NP, nanoparticle; i.t., intrathecally; GFAP, glial fibrillary acidic protein.

fluorescence after 24 hours treatment (Figure 3D). Also, cytotoxic effects of nanoparticles (0–200 μg/mL) were tested by MTT assay. Compared to PER without nanoparticles, there was no significant difference in cell viability (Figure 3E and F). Scanning electron microscopy showed that the material was composed of particles with a diameter <300 nm (Figure 3G). The drug release level from PLGA NPs was characterized in room temperature condition. The curve of the percentage of drug release from the total used drug in the synthesis process is shown in Figure 3H. The accumulation of PER release reached to 32.8% in day 5. Hence, this is considered as encapsulation efficiency of PER NPs.

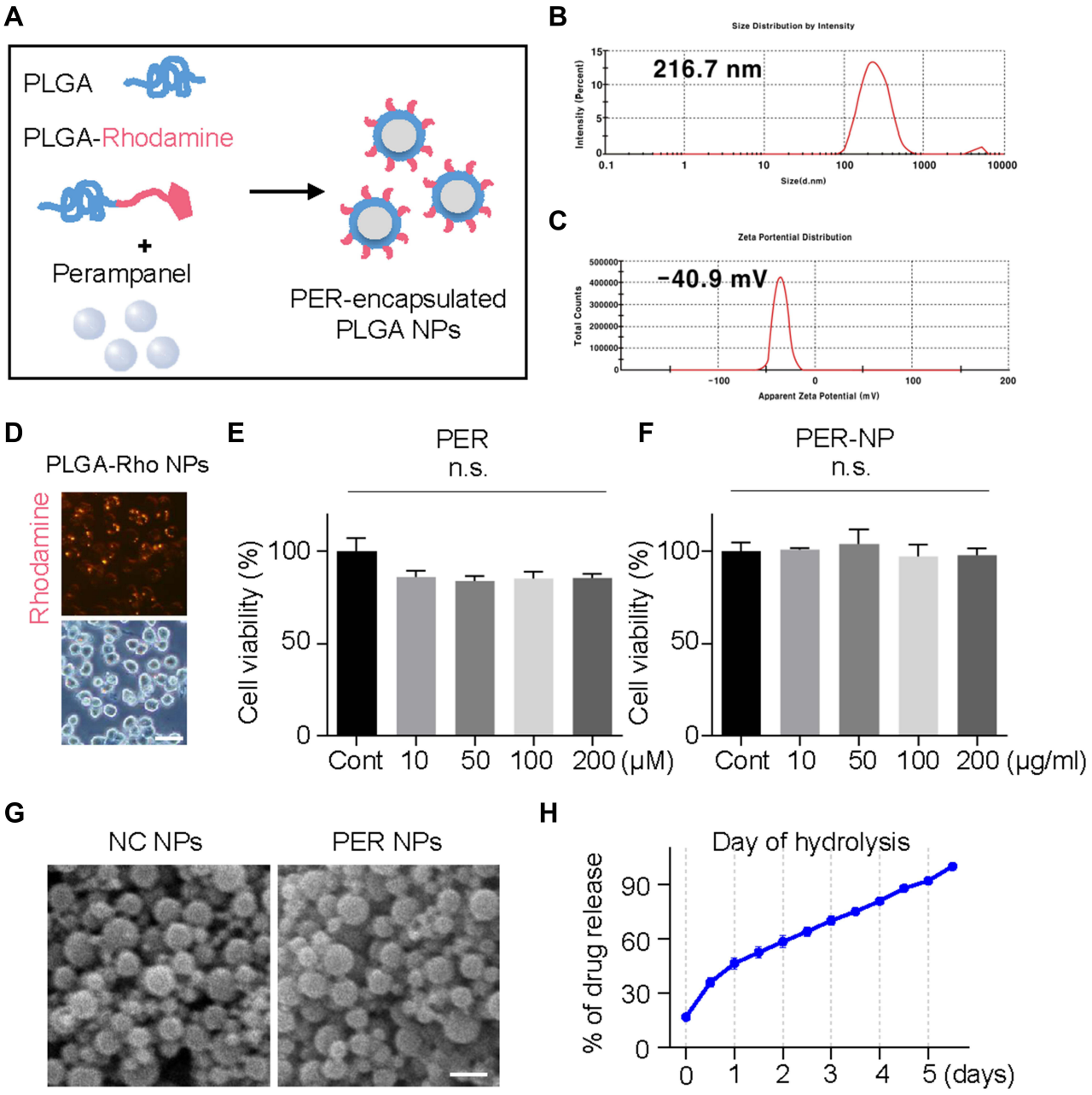

Figure 3 Characterization and cytotoxicity of PER encapsulated in PLGA NPs. (**A**) These PER-loaded PLGA NPs were prepared by sonicating a mixture of rhodamine-conjugated PLGA and PER. The NP size (**B**) and zeta potential (**C**) of the PER NPs. (**D**) BV2 cells were treated with Rho-PER NPs, and incubated for 3 hours. BV2 cells were incubated with PER itself (**E**) or PER NPs (**F**) for 24 hours. (**G**) Scanning electron microscopy images of nanoparticle films. Scale bar: 500 nm. (**H**) PER NPs were hydrolyzed by rolling in PBS for 5 days. The PER released into the suspension phase was observed by measuring the absorbance at a wavelength of 295 nm with a spectrometer.
Notes: (**E** and **F**) Data are expressed as mean ± SEM and analyzed by one-way ANOVA Tukey's post hoc test for multiple comparisons. n.s., not significant.
Abbreviations: PER, perampanel; PLGA, poly lactic-*co*-glycolic acid; NP, nanoparticle; SEM, standard error of mean; PBS, phosphate-buffered saline.

Intrathecal Injection of per NPs Attenuated Pro-Inflammatory Cytokine Release and Increased M2 Polarization of Microglia

According to a previous study that PER reduces cytokine release from microglia in adult stroke models, we investigated whether PER NPs could actually reduce microglial activation.[19] First, the PER NP-treated group showed significant improvements in the wire hang test compared with the negative control NP-treated group ($P = 0.0017$) (Figure 4A). Also, TTC staining showed a decreased infarct volume in the PER NP-treated group (Figure 4B and C). H&E staining revealed normal brain tissues in the NC NP or PER NP injected group, with uniform neuronal distribution. Neurons were rounded or oval, with pink cytoplasm, abundant and with clear nucleus. No inflammatory cells were detected. In the Rose Bengal model group, infarcted brain tissues were found, with a limited number of disordered neurons containing pale cytoplasm, eosinophils and abundance of vacuoles. In addition, a large infiltration of necrotic neurons and inflammatory cells was observed. However, we observed a significant decrease in tissues injected with PER NPs (Figure 4D). Further cell death morphology observed by staining the sections with cresyl violet showed necrotizing and pyknotic cells and apoptotic cells in the cortex region, suggesting that injection of PER NPs reduced apoptosis (Figure 4E). To measure the double-stranded cleavage of DNA, the TUNEL assay was performed in core infarcts at 24-h post stroke (Figure 4F). These data suggest that the brain tissue of rats injected with PER NPs has less extent of infarct and lee cell death. As activation of microglia leads to the release of pro-inflammatory cytokines in brain injury, we measured the mRNA levels of inflammatory genes. The levels of mRNA expression of TNF-α, IL-1β, COX2, and IL-6 significantly decreased in the PER NP-treated group compared with the control NP-treated group. However, there was no significant difference in the expression of iNOS (Figure 4G). Further, the PER NP-treated group showed markedly elevated protein expression of Ym1 and Arg1, markers for the M2 microglia phenotype (Figure 4H). Based on these results, it is likely that the blockade of AMPA receptors via PER NPs, which were distributed abundantly to the microglia, would affect M2 polarization and neuroprotective effects after perinatal stroke.

PER Protects Neuronal Cells by Increasing M2 Polarization in the Microglial BV2 Cell Line

Next, we investigated whether PER possibly increases M2 microglial polarization in vitro as well as in vivo. Preferentially, we examined dose-dependent cell death induced by treatment of BV2 cells with high to low concentrations, but there was no difference (Figure 5A). Then, we confirmed by Western blotting that the expression of the microglial M2 markers Arg1 and Ym1 increased in cells according to treatment with PER (Figure 5B). After PER treatment, the expression of Arg1 was increased at early time points, and the relative expression of Ym1 was induced on the third day. There was no significant change in the expression of Iba-1. Further, in order to model an actual inflammatory condition, the neuroinflammation was induced by lipopolysaccharide (LPS) treatment. BV2 cells were treated with varying doses of PER together with LPS (100 ng mL^{-1}) at the same time, and incubated for 1 day; treatment with LPS alone was used as a control. The levels of mArg1 were measured by qRT-PCR (Figure 5C). Following the application of LPS, the PER treatment restored expression of Arg1 compared to LPS alone.

Additionally, we tried to determine whether cobalt chloride ($CoCl_2$), a commonly used hypoxia analog, could increase Arg1 expression even when hypoxia is artificially induced.[29,30] To observe the effect of $CoCl_2$ treatment on inflammatory responses in microglia, BV2 cells were treated with PER and $CoCl_2$ (200 μM) for 24 hours (Figure 5D). The level of Arg1 expression also increased upon induction of the hypoxic condition by $CoCl_2$. These results suggest that PER strongly induced microglial M2 polarization. Because many studies have reported that, in neuroinflammation, microglia control neuronal death by cytokine secretion,[31,32] we questioned whether microglia had a significant effect on injured neurons under conditions of neonatal stroke. BV2 cells were co-treated with LPS, with or without PER, for 24 hours to prepare conditioned media (Figure 5E), and the media were used to treat HT22, a hippocampal neuron cell line, for 24 hours. The cytotoxicity toward HT22 cells was measured using an EZ-Cytox cell viability assay kit (Figure 5F). The cytotoxicity assay showed neuronal cell death, but it was confirmed that apoptosis decreased at higher concentrations of PER. These data demonstrate that PER has a neuroprotective effect by reducing the secretion of pro-inflammatory cytokines in microglia.

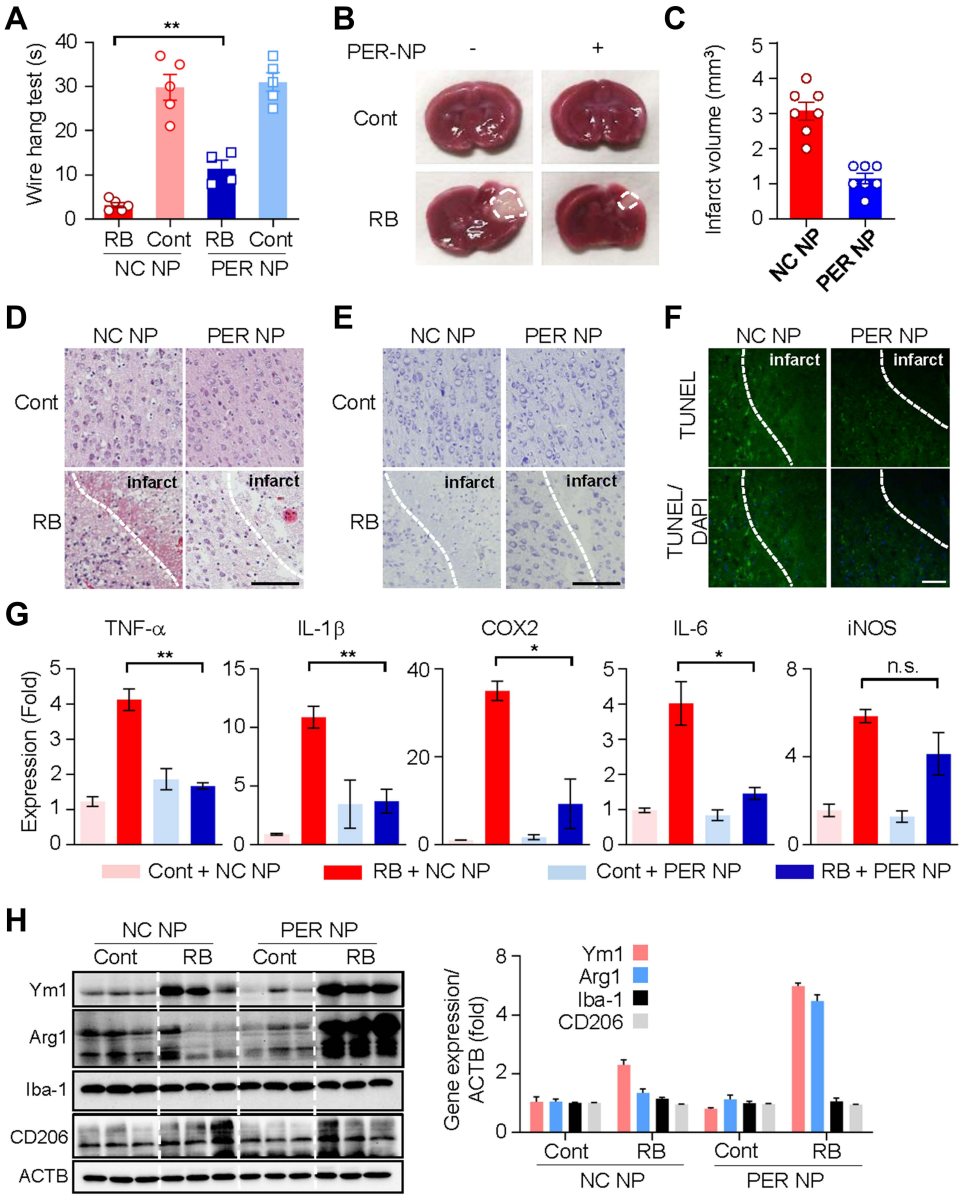

Figure 4 Microglia targeted by PER encapsulated in PLGA NPs attenuate infarct damage in the RB model, and reduce production of pro-inflammatory cytokines: (**A**) Wire hang test evaluated 24 h after RB photothrombosis. (**B**) Representative images of coronal brain sections stained with TTC. (**C**) Quantitative analysis of infarction volume. (**D**) Hematoxylin and eosin (H&E) staining of brain tissue sections of rat models of cerebral ischemia. Scale bar: 100 nm. (**E**) Cresyl violet staining of brain sections showed the infarct volume after 1 days of Rose Bengal modeling. Scale bar: 100 nm (**F**) Representative images of TUNEL staining in the cortical core infarct and penumbra within tissue collected after 24 h of Rose Bengal photothrombosis. Scale bar: 200 nm (**G**) The mRNA levels of TNF-α, IL-1β, Cox2, IL-6, and iNOS were measured using qRT-PCR. (**H**) Western blot analysis of Ym1, Arg1, Iba-1, CD206, and ACTB levels in cortical tissue of hemisphere subjected to 24 h of RB-induced photothrombosis.

Notes: (**A**) Data are expressed as mean ± SEM. **P = 0.0017 for RB/NC NP group vs RB/PER NP group. (**D**) On day 1 after RB modeling, total mRNA was extracted from the brain infarct region (0.7 cm) and used for cDNA synthesis. Data are presented as mean ± SEM. In one-way ANOVA with Tukey's post hoc test, **P = 0.0016, *P = 0.0130, n.s., not significant. (**G**) The integrated optical density of the protein band was calibrated relative to ACTB. Data are expressed as mean ± SEM.

Abbreviations: PER, perampanel; PLGA, poly lactic-co-glycolic acid; NP, nanoparticle; RB, Rose Bengal; TTC, Triphenyltetrazolium chloride; SEM, standard error of mean; ACTB, actin beta; NC, negative control.

Discussion

sThe purpose of this study was to evaluate the neuroprotective potential of PER, an AMPA receptor antagonist, in a rat neonatal stroke model. We used PLGA NPs for PER administration, to enhance delivery to microglia. Also, we demonstrated in this study that post-ischemic intrathecal administration of PER NPs, improved performance in the hanging test and induced M2 microglial activation. As a result, PER selectively delivered to microglia had a neuroprotective effect by reducing the secretion of pro-inflammatory cytokines and increasing microglia of the M2 phenotype.

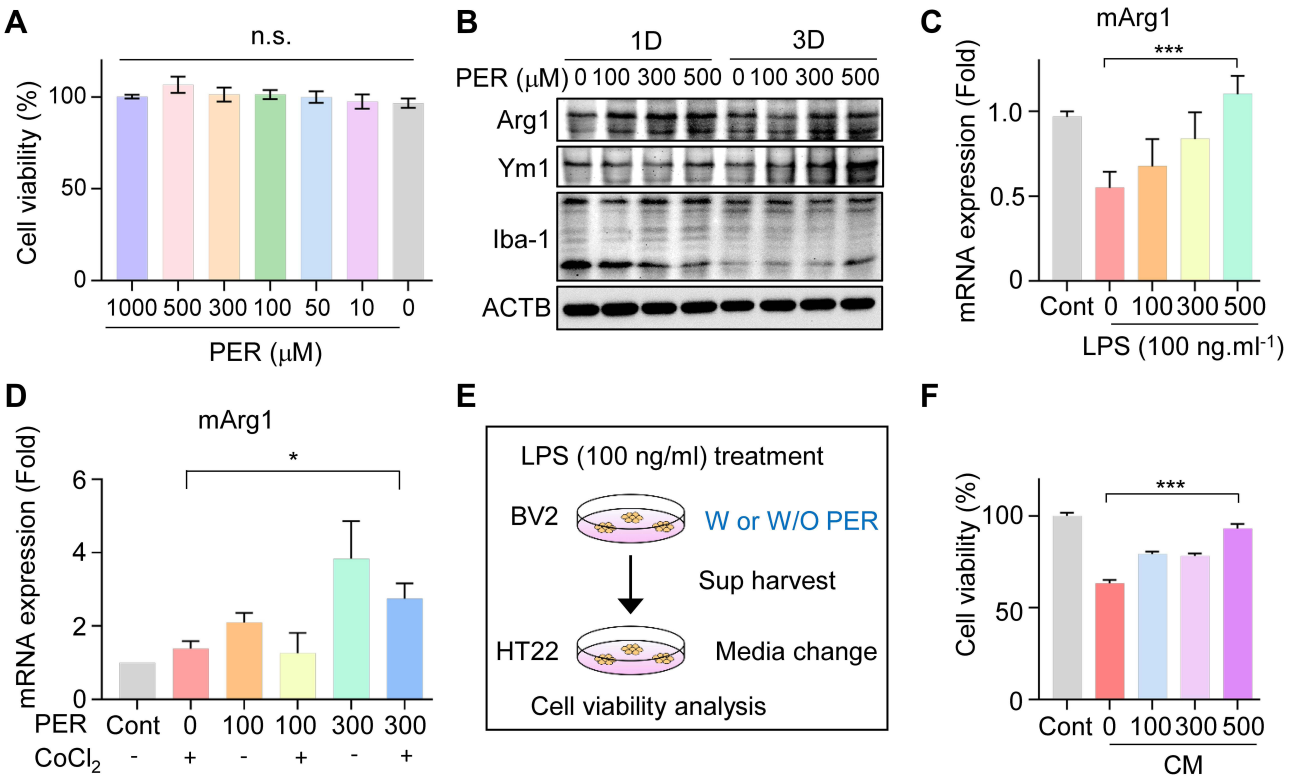

Figure 5 PER increases M2 microglial polarization and mediates neuroprotection in BV2 cells: (**A**) Dose-dependent cell viability was measured by treating with PER. (**B**) The related M2 microglial polarization was confirmed by Western blotting for Arg1, Ym1, and Iba-1 at 1 day and 3 days after PER treatment. (**C**) After PER treatment for 24 hours, mArg1 mRNA levels were checked in LPS-treated BV2 cells. (**D**) Microglial BV2 cells were co-treated with PER and $CoCl_2$, and incubated for 24 hours. Then, the mRNA level of Arg1 was measured by qRT-PCR in the absence or presence of PER. (**E**) BV2 cells were treated with LPS for 24 hours with and without PER to make CM and the medium was used to treat HT22. (**F**) Cytotoxicity after incubation of HT22 cells with BV2-CM for 24 hours.

Notes: (**A**) n.s., not significant. (**C**) Data are presented as mean ± SEM. In one-way ANOVA with Tukey's post hoc test, ***P = 0.0189 (**D**) Data are presented as mean ± SEM. In one-way ANOVA with Tukey's post hoc test, *P = 0.0402 for PER (300 μM)/$CoCl_2$ (200 μM) vs $CoCl_2$ (200 μM). (**E**) W or W/O, with or without (**F**) HT22 cells were incubated with BV2-CM for 24 hours. Data are presented as mean ± SEM. In one-way ANOVA with Tukey's post hoc test, ***P < 0.0001.

Abbreviations: PER, perampanel; LPS, lipopolysaccharide; CM, conditioned medium; SEM, standard error of mean.

Recent studies demonstrated that microglia have a broad range of effects in embryonic and postnatal physiological brain development, including regulation of embryonic vasculogenesis, secretion of trophic factors, immune surveillance, oligodendrogenesis, and neurogenesis.[33,34] They play key roles in establishing brain network connectivity during postnatal brain development. Moreover, microglia have been shown to regulate brain circuit connectivity in multiple ways. During embryonic neurogenesis, they regulate the stem cell pool via secretion of trophic factors and phagocytosis.[35] Phagocytosis of overproduced neurons and weakening of synapses by microglia, processes that govern brain connectivity, play important roles in organizing brain circuits during the postnatal period. The rodent brain at P7-P10 resembles 36–40 weeks of gestation in humans and thus is better suited for studying perinatal stroke at term.[36,37]

Microglia can be potent cellular targets for drug delivery, due to their role in propagating pathological processes after ischemic injury.[38] Microglial activation is the initial response in cerebral ischemia, and it is the primary source of cytokines and chemokines. Microglial polarization can be assessed by immunohistochemical analysis of specific markers. The activated microglia then produce detrimental pro-inflammatory cytokines (COX2, TNF-α, IL-1β and IL-6), which contribute to secondary brain ischemic injury and represent the main cause of cerebral injury aggravation.[39,40] It has been shown that M1 microglia promote secondary brain damage, whilst M2 microglia facilitate recovery following stroke.[6] Recently, questions have been raised about the usefulness of over-simplifying classification of microglia into the M1/M2 phenotypes.[36] However, what is still clear is that the repair phase begins after M1 microglial activation, and M2 microglia are the main cells with an anti-inflammatory immune response and can promote repair gene expression.[41]

Ischemic stroke results in energy depletion and ionic imbalance, followed by cell membrane depolarization, calcium overload, and extracellular accumulation of the excitatory amino acid glutamate. However, glutamate is also present at

a number of extra-synaptic locations, particularly those expressed by CNS glial cells.[22] Several previous studies showed that microglia contained mRNAs for GluR2-4 subunits of AMPA receptors.[28] Microglial AMPA receptor expression may be low or absent under healthy conditions, but may be induced in microglia activated under pathological conditions.[42] PER is a non-competitive AMPA receptor antagonist, which is now widely used as an adjuvant therapy in refractory epilepsy. Several previous studies showed the neuroprotective effect of PER after brain insult,[19,21] usually focused on neurons.[43] Various signaling pathways and multiple cellular and molecular changes have been shown, but most were side effects, and a detailed mechanism for this observation is still lacking. Up-regulated Ym1 expression is associated with reduced infarct sizes, and associated with improved neurological outcome and reduced neuronal cell death, according to previous studies.[44] Therefore, changing the activity of microglia may be one of the pathways available for neuroprotective strategies.

A promising strategy for microglia-targeted therapeutic development is the delivery of drugs via nanoparticles. Nanoparticle-based drug delivery systems present great potential, due to their flexibly manipulated physical and chemical properties, and provide unique solutions to the problem of BBB penetration. PLGA NPs distribute to microglia, so the study using PER-loaded NPs could tell particularly well the effect of PER on microglia. Our findings postulate a beneficial therapeutic effect in perinatal stroke patients with alteration of the microglial phenotype. However, although these nanoparticles have excellent ability to deliver drug, several questions remain to be addressed, including (1) how PER NPs actually act on microglia, and whether their action is limited only to acute phase, and (2) how M2 polarization can attenuate infarction volume. In order to find answers to these questions, further experimental studies on the effects of PER on microglial activation are needed. Although we cannot determine the exact mechanism by which PER-PLGA nanoparticles affected microglial polarity in this study, it is obvious that blocking microglial AMPA receptors during the early stage post-stroke could be effective for the treatment of ischemic stroke. Therefore, for neonatal stroke, PER-based nanopharmaceuticals could be promising treatments to be investigated in future clinical research. In conclusion, the present study showed that PER-loaded nanoparticles have neuroprotective effects via M2 microglial polarization in a rat model of perinatal stroke.

Nanotechnology could be defined as the vehicle to enhance the therapeutic efficacy of loaded drugs as various nanomaterials are being developed for use in a new generation of drug delivery systems.[45] The development of a wide spectrum of nanoscale technologies is beginning to change the scientific landscape in terms of disease diagnosis, treatment, and prevention. Biodegradable polymers have been studied extensively over the past few decades for the fabrication of drug delivery systems. PLGA applied in our study is one of the nanomaterials, a copolymer as a drug delivery. Moreover, PLGA nanoparticles have the advantages of low cost, stability, and biodegradability, and it has been confirmed in previous studies that they preferentially uptake by microglia. The uptake efficiency of microglia is more stronger than astrocyte or neuron by 50% or more.[8,11] The PLGA nanoparticles follow is of a 'typical" endocytosis-exocytosis route.[46] In summary, as we can expect, it is a delivery system in which PLGA nanoparticles are up-taken through cellular endocytosis, and the encapsulated DNA is delivered to the cell as PLGA is biodegraded.

Pharmacotherapy for ischemic stroke has limitations, and in order to achieve the therapeutic effect of the drug, it is necessary to study the mechanism of passage through the BBB. The BBB is a barrier between the nervous system and other parts of the body that can protect the brain from harmful stimuli, but also interferes with the delivery of drugs that need to be delivered to the brain. Therefore, it is difficult for existing drugs to pass through the BBB. Nanomedicines can be actively transported by transcytosis, thereby improving BBB transport and improving drug permeability.[47] Among them, the PLGA nanoparticles we used a kind of polymeric nanocarrior can carry hydrophilic reagents and they can internalize drugs into cells via endocytosis. Moreover, PLGA nanoparticles consist of single-particle, they have the advantage of having an extremely small modal volume and the potential to reach ultra-high Purcell factors.[48]

A recently reported concept, two-dimensional (2D) monoelemental materials, Xenes has advanced into the development of inorganic and organic nanostructures for imaging, sensing and targeted delivery of therapeutics for biomedical applications.[49] Xenes have already shown promise for various biomedical applications. The scope of biomedical applications can be further expanded by making the best of the optical properties, induced magnetic characteristic of Xenes, and rational surface modification with drugs, photosensitizers, imaging, and sensing agents. We expect that good

results will be obtained if we apply Xenes to PLGA nanoparticles used for drug delivery in the future and apply it to follow-up study.

Conclusion

In this study, we investigated the effect of PER-loaded PLGA by targeting microglia in perinatal stroke. After formation of focal ischemic stroke by photothrombosis in P7 rats, PER-loaded PLGA was injected intrathecally. Proinflammatory markers (TNF-α, IL-1β, IL-6, COX2, and iNOS) and M2 polarization markers (Ym1 and Arg1) were evaluated. We investigated whether PER increased M2 microglial polarization in vitro. PER-loaded PLGA nanoparticles decreased the pro-inflammatory cytokines compared to the control group. Furthermore, they increased M2 polarization. The development of a drug delivery system targeting microglia confirms the potential to develop new therapeutic agents for perinatal ischemic stroke.

Acknowledgment

This research was funded by the National Research Foundation of Korea (NRF-2020R1C1C1007488, NRF-2020R1l1A1A0105309611, and NRF- 2021R1C1C2007218).

Disclosure

The authors report no conflicts of interest in this work.

References

1. Nelson KB, Lynch JK. Stroke in newborn infants. *Lancet Neurol*. 2004;3(3):150–158. doi:10.1016/S1474-4422(04)00679-9
2. Fernandez-Lopez D, Natarajan N, Ashwal S, Vexler ZS. Mechanisms of perinatal arterial ischemic stroke. *J Cereb Blood Flow Metab*. 2014;34(6):921–932. doi:10.1038/jcbfm.2014.41
3. Ko SB, Park HK, Kim BM, et al. 2019 Update of the Korean clinical practice guidelines of stroke for endovascular recanalization therapy in patients with acute ischemic stroke. *Neurointervention*. 2019;14(2):71–81. doi:10.5469/neuroint.2019.00164
4. Murphy A, Symons SP, Hopyan J, Aviv RI. Factors influencing clinically meaningful recanalization after IV-rtPA in acute ischemic stroke. *AJNR Am J Neuroradiol*. 2013;34(1):146–152. doi:10.3174/ajnr.A3169
5. Ferriero DM, Fullerton HJ, Bernard TJ, et al. Management of stroke in neonates and children: a scientific statement from the American association/American Stroke Association. *Stroke*. 2019;50(3):e51–e96.
6. Jiang CT, Wu WF, Deng YH, Ge JW. Modulators of microglia activation and polarization in ischemic stroke. *Mol Med Rep*. 2020;21(5):2006–2018. doi:10.3892/mmr.2020.11003
7. Meng HL, Li XX, Chen YT, et al. Neuronal soluble fas ligand drives M1-microglia polarization after cerebral ischemia. *CNS Neurosci Ther*. 2016;22(9):771–781. doi:10.1111/cns.12575
8. Kim SI, Shin J, Tran Q, et al. Application of PLGA nanoparticles to enhance the action of duloxetine on microglia in neuropathic pain. *Biomater Sci-UK*. 2021;9(18):6295–6307. doi:10.1039/D1BM00486G
9. Li JY, Sabliov C. PLA/PLGA nanoparticles for delivery of drugs across the blood-brain barrier. *Nanotechnol Rev*. 2013;2(3):241–257. doi:10.1515/ntrev-2012-0084
10. Shin HJ, Park H, Shin N, et al. p47phox siRNA-Loaded PLGA nanoparticles suppress ROS/oxidative stress-induced chondrocyte damage in osteoarthritis. *Polymers-Basel*. 2020;12(2):443.
11. Shin J, Yin Y, Park H, et al. p38 siRNA-encapsulated PLGA nanoparticles alleviate neuropathic pain behavior in rats by inhibiting microglia activation. *Nanomedicine-UK*. 2018;13(13):1607–1621. doi:10.2217/nnm-2018-0054
12. Shin N, Shin HJ, Yi Y, et al. p66shc siRNA-encapsulated PLGA nanoparticles ameliorate neuropathic pain following spinal nerve ligation. *Polymers-Basel*. 2020;12(5):1014.
13. Garcia-Corvillo MD. Polymeric nanoparticles for drug delivery to the central nervous system via nasal route. *Ars Pharm*. 2016;57(1):27–35.
14. Lee S, Shin HJ, Noh C, et al. IKBKB siRNA-encapsulated poly (Lactic-co-Glycolic Acid) nanoparticles diminish neuropathic pain by inhibiting microglial activation. *Int J Mol Sci*. 2021;22(11):5657.
15. Pham TL, Yin Y, Kwon HH, et al. miRNA 146a-5p-loaded poly(d,l-lactic-co-glycolic acid) nanoparticles impair pain behaviors by inhibiting multiple inflammatory pathways in microglia. *Nanomedicine-UK*. 2020;15(11):1113–1126. doi:10.2217/nnm-2019-0462
16. Hanada T, Hashizume Y, Tokuhara N, et al. Perampanel: a novel, orally active, noncompetitive AMPA-receptor antagonist that reduces seizure activity in rodent models of epilepsy. *Epilepsia*. 2011;52(7):1331–1340. doi:10.1111/j.1528-1167.2011.03109.x
17. Krauss GL, Serratosa JM, Villanueva V, et al. Randomized Phase III study 306 adjunctive perampanel for refractory partial-onset seizures. *Neurology*. 2012;78(18):1408–1415. doi:10.1212/WNL.0b013e318254473a
18. French JA, Krauss GL, Steinhoff BJ, et al. Evaluation of adjunctive perampanel in patients with refractory partial-onset seizures: results of randomized global phase III study 305. *Epilepsia*. 2013;54(1):117–125. doi:10.1111/j.1528-1167.2012.03638.x
19. Nakajima M, Suda S, Sowa K, et al. AMPA receptor antagonist perampanel ameliorates post-stroke functional and cognitive impairments. *Neuroscience*. 2018;386:256–264. doi:10.1016/j.neuroscience.2018.06.043
20. Niu HX, Wang JZ, Wang DL, et al. The orally active noncompetitive AMPAR antagonist perampanel attenuates focal cerebral ischemia injury in rats. *Cell Mol Neurobiol*. 2018;38(2):459–466. doi:10.1007/s10571-017-0489-x

21. Chen T, Dai SH, Jiang ZQ, et al. The AMPAR antagonist perampanel attenuates traumatic brain injury through anti-oxidative and anti-inflammatory activity. *Cell Mol Neurobiol*. 2017;37(1):43–52. doi:10.1007/s10571-016-0341-8
22. Ceprian M, Fulton D. Glial cell ampa receptors in nervous system health, injury and disease. *Int J Mol Sci*. 2019;20(10):2450. doi:10.3390/ijms20102450
23. Yi YY, Shin HJ, Choi SG, et al. Preventive effects of neuroprotective agents in a neonatal rat of photothrombotic stroke model. *Int J Mol Sci*. 2020;21(10):3703. doi:10.3390/ijms21103703
24. Maji R, Dey NS, Satapathy BS, Mukherjee B, Mondal S. Preparation and characterization of Tamoxifen citrate loaded nanoparticles for breast cancer therapy. *Int J Nanomedicine*. 2014;9:3107–3118. doi:10.2147/IJN.S63535
25. Kang J, Park EJ, Jou I, Kim JH, Joe EH. Reactive oxygen species mediate A beta (25–35)-induced activation of BV-2 microglia. *Neuroreport*. 2001;12(7):1449–1452. doi:10.1097/00001756-200105250-00030
26. Blasi E, Barluzzi R, Bocchini V, Mazzolla R, Bistoni F. Immortalization of murine microglial cells by a v-raf/v-myc carrying retrovirus. *J Neuroimmunol*. 1990;27(2–3):229–237. doi:10.1016/0165-5728(90)90073-V
27. Hwang JA, Shin N, Shin HJ, et al. Protective effects of ShcA protein silencing for photothrombotic cerebral infarction. *Transl Stroke Res*. 2021;12(5):866–878. doi:10.1007/s12975-020-00874-1
28. Noda M, Nakanishi H, Nabekura J, Akaike N. AMPA-kainate subtypes of glutamate receptor in rat cerebral microglia. *J Neurosci*. 2000;20(1):251–258. doi:10.1523/JNEUROSCI.20-01-00251.2000
29. Kim EH, Won JH, Hwang I, Yu JW. Cobalt chloride-induced hypoxia ameliorates NLRP3-mediated caspase-1 activation in mixed glial cultures. *Immune Netw*. 2013;13(4):141–147. doi:10.4110/in.2013.13.4.141
30. Peng X, Li C, Yu W, et al. Propofol attenuates hypoxia-induced inflammation in BV2 microglia by inhibiting oxidative stress and NF-kappaB/Hif-1alpha signaling. *Biomed Res Int*. 2020;2020:8978704. doi:10.1155/2020/8978704
31. Wang WY, Tan MS, Yu JT, Tan L. Role of pro-inflammatory cytokines released from microglia in Alzheimer's disease. *Ann Transl Med*. 2015;3(10):136. doi:10.3978/j.issn.2305-5839.2015.03.49
32. Harry GJ, Kraft AD. Neuroinflammation and microglia: considerations and approaches for neurotoxicity assessment. *Expert Opin Drug Metab Toxicol*. 2008;4(10):1265–1277. doi:10.1517/17425255.4.10.1265
33. Murabe Y, Sano Y. Morphological studies on neuroglia. V. Microglial cells in the cerebral cortex of the rat, with special reference to their possible involvement in synaptic function. *Cell Tissue Res*. 1982;223(3):493–506. doi:10.1007/BF00218471
34. Dalmau I, Finsen B, Zimmer J, Gonzalez B, Castellano B. Development of microglia in the postnatal rat hippocampus. *Hippocampus*. 1998;8(5):458–474. doi:10.1002/(SICI)1098-1063(1998)8:5<458::AID-HIPO6>3.0.CO;2-N
35. Cunningham CL, Martinez-Cerdeno V, Noctor SC. Microglia regulate the number of neural precursor cells in the developing cerebral cortex. *J Neurosci*. 2013;33(10):4216–4233. doi:10.1523/JNEUROSCI.3441-12.2013
36. Mallard C, Tremblay ME, Vexler ZS. Microglia and neonatal brain injury. *Neuroscience*. 2019;405:68–76. doi:10.1016/j.neuroscience.2018.01.023
37. Paolicelli RC, Bolasco G, Pagani F, et al. Synaptic pruning by microglia is necessary for normal brain development. *Science*. 2011;333(6048):1456–1458. doi:10.1126/science.1202529
38. Joseph A, Liao R, Zhang MY, et al. Nanoparticle-microglial interaction in the ischemic brain is modulated by injury duration and treatment. *Bioeng Transl Med*. 2020;5(3). doi:10.1002/btm2.10175
39. Peng JH, Pang JW, Huang L, et al. LRP1 activation attenuates white matter injury by modulating microglial polarization through Shc1/PI3K/Akt pathway after subarachnoid hemorrhage in rats. *Redox Biol*. 2019;21:101121. doi:10.1016/j.redox.2019.101121
40. Wang XY, Chen SS, Ni JS, Cheng J, Jia J, Zhen XC. miRNA-3473b contributes to neuroinflammation following cerebral ischemia. *Cell Death Dis*. 2018;9:1–3.
41. Tang Y, Le WD. Differential roles of M1 and M2 microglia in neurodegenerative diseases. *Mol Neurobiol*. 2016;53(2):1181–1194. doi:10.1007/s12035-014-9070-5
42. Gottlieb M, Matute C. Expression of ionotropic glutamate receptor subunits in glial cells of the hippocampal CA1 area following transient forebrain ischemia. *J Cerebr Blood F Met*. 1997;17(3):290–300. doi:10.1097/00004647-199703000-00006
43. Mazzocchetti P, Mancini A, Sciaccaluga M, et al. Low doses of Perampanel protect striatal and hippocampal neurons against in vitro ischemia by reversing the ischemia-induced alteration of AMPA receptor subunit composition. *Neurobiol Dis*. 2020;140:104848. doi:10.1016/j.nbd.2020.104848
44. Collmann FM, Pijnenburg R, Hamzei-Taj S, et al. Individual in vivo profiles of microglia polarization after stroke, represented by the genes iNOS and Ym1. *Front Immunol*. 2019;10. doi:10.3389/fimmu.2019.01236
45. Singh R, Lillard JW Jr. Nanoparticle-based targeted drug delivery. *Exp Mol Pathol*. 2009;86(3):215–223. doi:10.1016/j.yexmp.2008.12.004
46. Cartiera MS, Johnson KM, Rajendran V, Caplan MJ, Saltzman WM. The uptake and intracellular fate of PLGA nanoparticles in epithelial cells. *Biomaterials*. 2009;30(14):2790–2798. doi:10.1016/j.biomaterials.2009.01.057
47. Tian X, Fan T, Zhao W, et al. Recent advances in the development of nanomedicines for the treatment of ischemic stroke. *Bioact Mater*. 2021;6(9):2854–2869. doi:10.1016/j.bioactmat.2021.01.023
48. Azzam SI, Kildishev AV, Ma RM, et al. Ten years of spasers and plasmonic nanolasers. *Light Sci Appl*. 2020;9:90. doi:10.1038/s41377-020-0319-7
49. Xie Z, Zhang B, Ge Y, et al. Chemistry, functionalization, and applications of recent monoelemental two-dimensional materials and their heterostructures. *Chem Rev*. 2022;122(1):1127–1207. doi:10.1021/acs.chemrev.1c00165